relative error in the determined apparent molecular weight MW is, roughly, for small Mach number

$$\Delta(MW)/MW \simeq [T_o/(T_w - T_o) - 2]M^2 \quad (5)$$

or less, if γ and α vary with concentration.

8. Time Response

As the distance from the orifice in the tip to the wire is small and the gas velocity is of the order of the speed of sound a time response of μsec might be expected, unless the size of the hot wire and the electronics limit it to a longer time.

A new probe with a smaller wire diameter (0.0001 in.) and a less rapid area expansion (based on the findings in Sec. 6) was constructed and placed in the end wall of a shock tube. The gas in the tube was nitrogen, initially at atmospheric pressure. A shock wave passing by the probe produced an instantaneous change in the stagnation conditions of the sampled gas and the corresponding change in probe output was photographed (Fig. 6), (time scale = 100 μsec/cm, vertical scale = 0.05 v/cm). The response time is evidently about 200 μsec. The experiment was repeated using helium instead of nitrogen and, as expected, the rise time was faster. It is noted that a much longer time response is associated with the warming up of the glass.

References

[1] Blackshear, Perry L. and Lingerson, Leroy, "Rapid-Response Heat Flux Probe for High Temperature Gases," *ARS Journal*, Vol. 32, No. 1, Nov. 1962, pp. 1709–1715.

[2] D'Souza, Gerard J., Montealegre, Anthony, and Weinstein, Herbert, "Measurement of Turbulent Correlations in a Coaxial Flow of Dissimilar Fluids," CR-970, Jan. 1968, NASA.

[3] Baldwin, L. V., Sandborn, V. A., and Laurence, J. C., "Heat-Transfer from Transverse and Yawed Cylinders in Continuum, Slip and Free Molecule Air Flows," *Journal of Heat Transfer*, Vol. 82, No. 1, May 1960, pp. 77–86.

[4] Aihara, Y., Kassoy, D. R., and Libby, Paul A., "Heat Transfer from Circular Cylinders at Low Reynolds Numbers," *The Physics of Fluids*, Vol. 10, No. 1, May 1967, pp. 947–952.

[5] Loeb, Leonard B., "The Laws of Rarefied Gases and Surface Phenomena," *The Kinetic Theory of Gases*, 3rd ed., Dover, 1961, pp. 278–364.

[6] Faust, J. W., "Accommodation Coefficient of Inert Gases on Al and Pt and Their Dependence on Surface Condition," Ph.D. thesis, 1954, Univ. of Missouri, Columbia, Mo.

[7] Dewey, C. Forbes, Jr., "A Correlation of Convective Heat Transfer and Recovery Temperature Data for Cylinders in Compressible Flow," *International Journal of Heat and Mass Transfer*, Vol. 8, No. 1, Feb. 1965, pp. 245–252.

[8] Brown, G. L., and Roshko, Anatol, "The Effect of Density Differences on the Turbulent Mixing Layer," AGARD Conference Proceedings Turbulent Shear Flows, Nov. 1971, to be published.

MAY 1972 AIAA JOURNAL VOL. 10, NO. 5

Supersonic Interaction in the Corner of Intersecting Wedges at High Reynolds Numbers

JOHN E. WEST* AND ROBERT H. KORKEGI†
Aerospace Research Laboratories, Wright-Patterson AFB, Ohio

The flow structure was determined in the streamwise corner formed by two intersecting wedges of 9½° half-angle in a supersonic stream at a Mach number of 3, and over a Reynolds number range from 0.4 to 60 × 10^6. Measurements included Pitot traverses, surface pressures, and oil flow visualization. For Reynolds numbers below 3 × 10^6 the wedge boundary layer was first laminar, then transitional, and the corner interaction initially extended laterally well beyond the embedded shock. For Reynolds numbers greater than 3 × 10^6 for which the boundary layer was turbulent, the interaction region barely extended beyond the embedded shock and the flow structure was found to be conically invariant and therefore essentially independent of viscous effects. Spanwise surface pressure distributions for both the laminar and the turbulent cases are virtually identical to those for two-dimensional flow separation.

Nomenclature

x = axial distance normal to the plane formed by the model leading edges (in.)
y = vertical distance normal to x, measured from the intersection of the wedges (in.)
z = horizontal distance normal to x, measured from the intersection of the wedges (in.)
p = pressure (psia)
p_t = Pitot pressure (psia)
M = Mach number
Re = local Reynolds number based on undisturbed wedge conditions

Subscripts

w = two-dimensional wedge conditions
∞ = freestream conditions
o = stagnation conditions

Received August 18, 1971; revision received October 29, 1971.

* Major USAF, Aerospace Engineer, Hypersonic Research Laboratory. Member AIAA.

† Director, Hypersonic Research Laboratory. Associate Fellow AIAA.

Introduction

THE flow structure in a corner of intersecting wedges at supersonic speeds was first found experimentally by Charwat and Redekopp.[1] Their study revealed that the wedge bow shocks do not intersect, but rather, are joined by a third corner shock, and the internal flow includes two embedded shocks which terminate at the wedge surfaces, and a triangular region bounded by two slip surfaces and the corner shock. Subsequent studies with intersecting wedges[2,3] and flat plates[4] in hypersonic streams showed a similar corner flow structure.

Aside from a few turbulent surface heat transfer measurements by Stainbach and Weinstein[5] all experimental studies of corner interaction in supersonic and hypersonic flow were carried out at relatively low Reynolds numbers for which boundary layers were laminar. Thus, displacement effects, particularly in the forward region of the model, as well as viscous-inviscid interactions could be expected to influence the entire inviscid flow structure far downstream. Furthermore, experiments[1,5] revealed a considerable spread of disturbed flow extending laterally from the corner intersection far beyond the location of the embedded shock. The

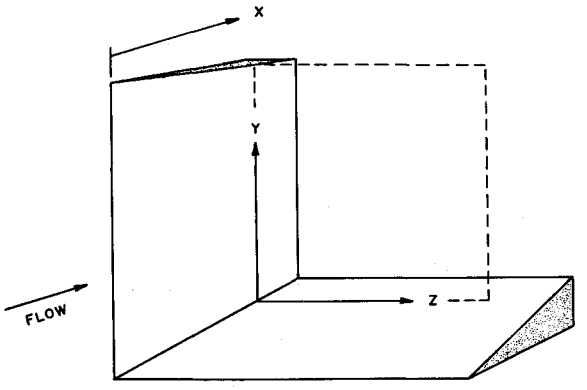

Fig. 1 Model coordinate system.

second author has suggested[6] that this outer region reflects boundary layer separation and not an inviscid interaction as was first believed.[1]

Theoretical prediction methods are far from adequate. Some local properties of a supersonic corner interaction are calculated by Goebel[7] and a merged layer approach applicable to hypersonic flows at low Reynolds numbers is given by Rubin.[4] However, there is presently no method of prediction of even the inviscid corner flow structure with its embedded shocks and slipstreams.[6]

The present investigation of corner flow at Mach number 3 and high Reynolds numbers had for objectives to minimize boundary-layer displacement effects so that the corner flow structure away from the walls is essentially inviscid and therefore conical, and to determine viscous-inviscid interaction with a fully developed turbulent boundary layer. A more extensive discussion of this work is given in Ref. 8.

Experimental Equipment and Techniques

The study was carried out in the Aerospace Research Laboratory's 8 in. × 8 in. Mach 3 high Reynolds number facility over a stagnation pressure range from 4.2 to 570 psia providing a unit Reynolds number variation from 0.8 to 113 × 10^6/ft.

The basic model consisted of two stainless steel nominal 10° sharp wedged (leading-edge radius ~0.0005 in.) each of 6-in. span and 5-in. chord, intersecting at right angles. The model was aligned in the tunnel test section to yield equal pressures on both wedges. The resulting value was $p_w/p_\infty = 1.98$ corresponding to effective wedge angles of 9.5° for $M = 3$. The horizontal wedge contained two flush-mounted phosphor bronze sliders with centerlines at $x = 1.71$ and 3.45 in. respectively. The sliders could be fitted with either surface pressure taps or dogleg Pitot tubes of various heights in order to survey the complete corner interaction region. The sliders provided a continuous trace of pressures, and their position was given by a linear potentiometer accurate within ±0.01 in. Pressures were measured with variable reluctance pressure transducers of appropriate ranges, and the output recorded on an $x - y$ plotter, with slider position as the abscissa. Over-all accuracy of measurement was ±5% for the surface pressure ratio p/p_w and ±2% for the ratio of Pitot to stagnation pressure p_t/p_o. The coordinate system for presentation of the results is shown in Fig. 1.

Oil flow studies were made on the vertical wedge. Best results were obtained with a mixture of 10 mliters of 5 centistoke silicone oil, 1.5 g of titanium dioxide, and 10 drops of oleic acid.

Corner Flow Structure

The turbulent corner flow structure shown in Fig. 2 was determined from Pitot pressure surveys mapping out the corner region. Qualitatively the structure is similar to that found by Charwat and Redekopp[1] and other investigators[2,4] in that it consists of an oblique corner shock joining the two wedge shocks, embedded shocks from the two shock intersection points toward the wedge surfaces; and from these same two points, slipstreams which converge toward the intersection of the wedges and which separate the flow crossing the corner shock from that crossing the two wedge and embedded shocks.

The flow structure was constructed from Pitot surveys over a range of Re from 3 to 37 × 10^6, achieved by varying p_o by a

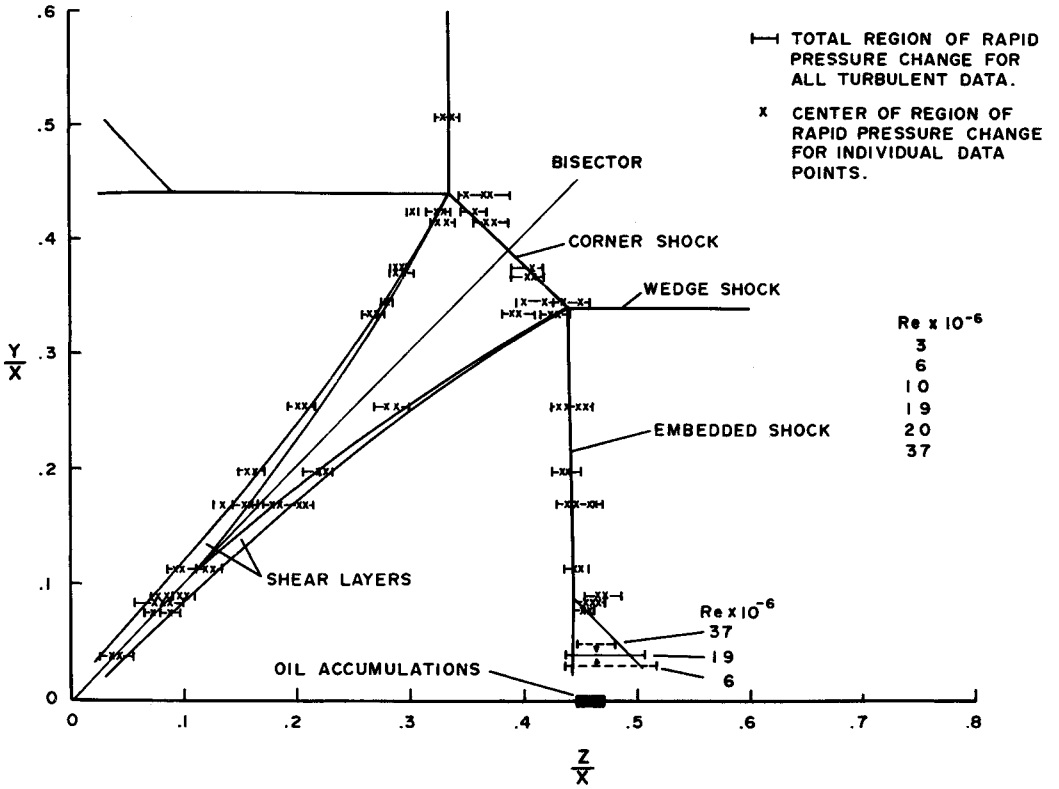

Fig. 2 Flow structure for the turbulent case with data for a wide range of Re's.

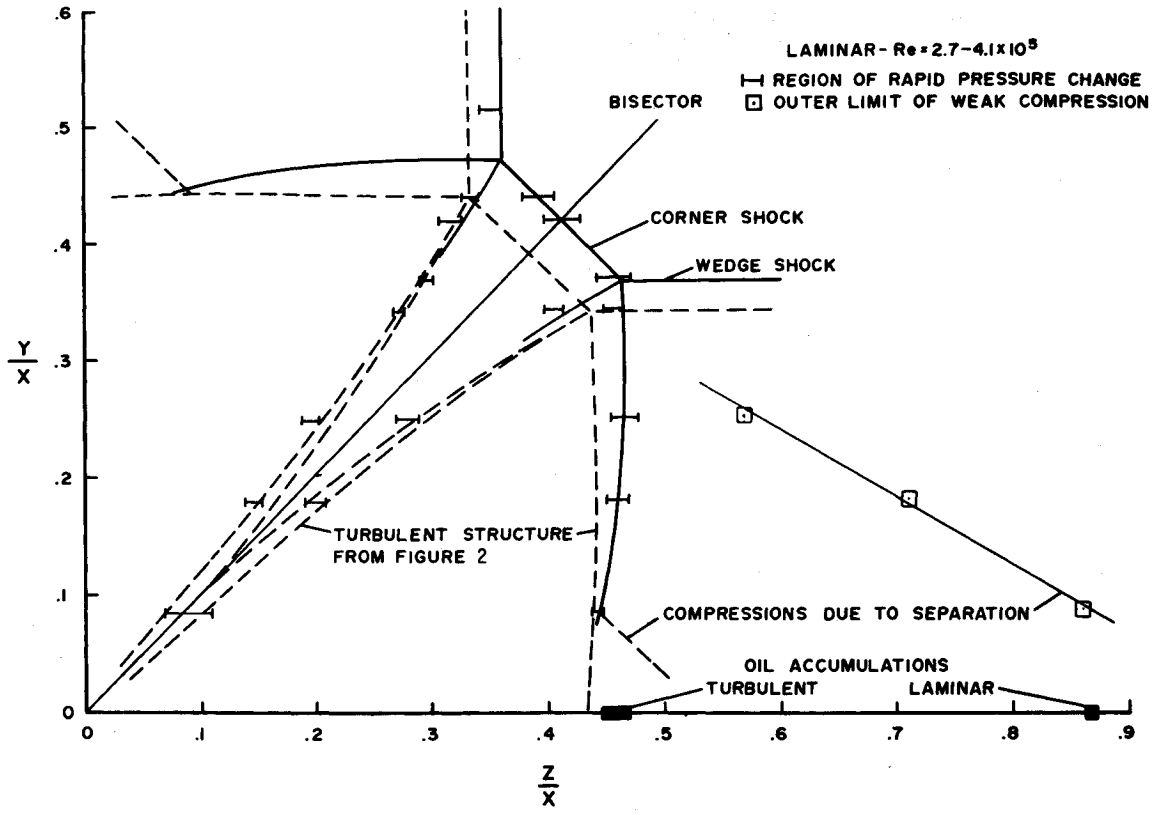

Fig. 3 Flow structure for a particular laminar case compared with the turbulent structure.

factor of 6 and x by a factor of 2. The short horizontal traces of Fig. 2 represent the extent of the regions of rapid Pitot pressure rise or drop. The striking feature of Fig. 2 is that there is no measurable Reynolds number effect over this wide range of Re; slight variations in location of shocks and slipstreams are random and attributed to experimental error. Slight departures occur only at the foot of the embedded shock where the compression zone has a small lateral spread which grows with decreasing Reynolds number. Also shown is the position of the oil accumulation line (see next section) given as a band to reflect its slight variation over the Re range in accordance with the slight spread of the compression zone. The oil accumulation reflects a line of flow separation due to the impingement of the embedded shock on the wedge boundary layer.

Hence, with the exception of a small region near the foot of the embedded shocks, the configuration of Fig. 2 is considered to represent the inviscid flow structure in a symmetrical axial corner for wedge angles of 9.5° and a freestream Mach number of 3.

Outboard of the embedded shock there is no sign of a disturbance such as found by Charwat and Redekopp[1] (their Region III). Between the embedded shock and the slipstream, the Pitot pressure increases gradually from the wedge surface to the shock intersection point where it is approximately 5% higher. This could be accounted for by a very slight concave curvature of the embedded shock, opposite in shape and considerably less pronounced than that given in Ref. 1. In the triangular region between the slipstreams there is a slight decrease in Pitot pressure by about 5% from the corner shock radially inward.

The slipstreams, or free shear layers, start with zero thickness at the triple point and grow in width toward the corner intersection to eventually merge with each other at about $\frac{1}{4}$ the distance from the wedge intersection to the corner shock. This growth follows from the fact that, as one moves in toward the corner intersection, successive layers of the slipstreams have originated further upstream than the previous ones.

The corner interaction region is markedly smaller than that found by Charwat and Redekopp[1] even accounting for small differences in Mach number (3 instead of 3.17) and wedge angle (9.5° instead of 12.2°), but their Re's were low—$\leq 0.2 \times 10^6$. As a means of comparison, measurements were made at a Re of 0.39×10^6 for which the boundary layer was known to be laminar. The resulting flow structure, shown in Fig. 3, differs markedly from that of Fig. 2. It is now clear that significant

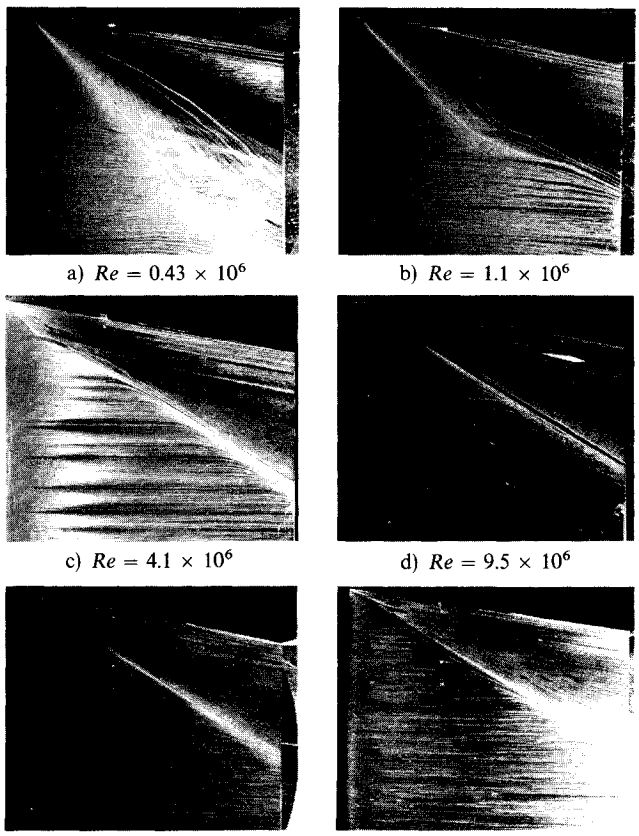

a) $Re = 0.43 \times 10^6$ b) $Re = 1.1 \times 10^6$

c) $Re = 4.1 \times 10^6$ d) $Re = 9.5 \times 10^6$

e) $Re = 30 \times 10^6$ f) $Re = 60 \times 10^6$

Fig. 4 Surface oil flow patterns for a wide range of Re.

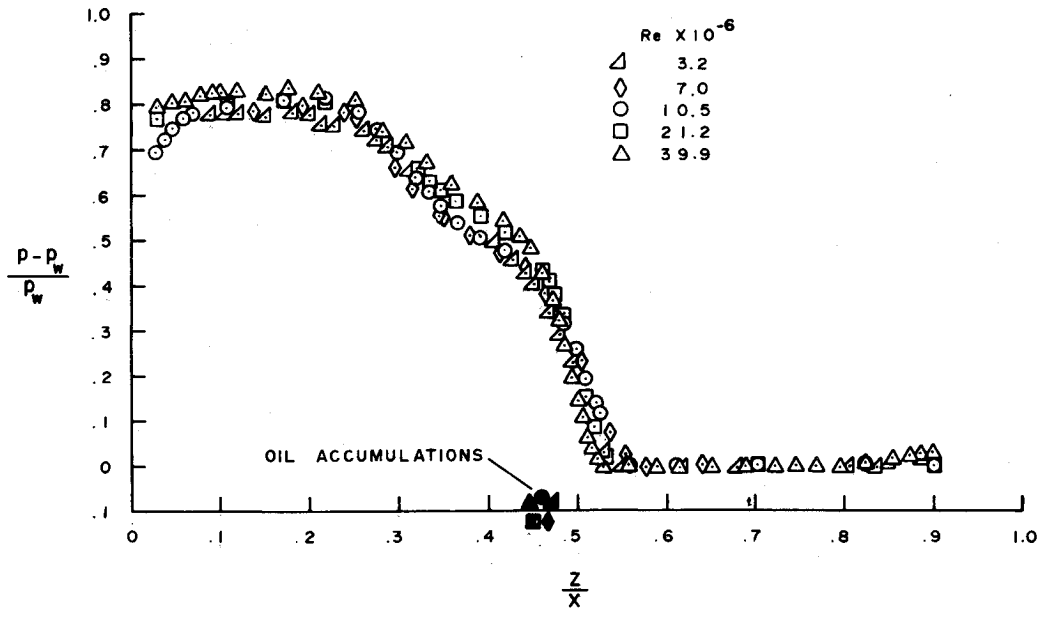

Fig. 5 Surface pressure distributions corresponding to high *Re*.

viscous influences in the form of boundary-layer displacement effects and strong laminar viscous-inviscid interactions are present at low *Re*. The present measurements indicate that an invariant conical pattern is obtained only for *Re* numbers greater than 3×10^6 for the configuration and conditions of the present test.

Corner Flow Surface Interactions

The dominant effect of the boundary layer and hence the viscous-inviscid interaction, in determining the surface flow pattern and pressure distribution is quite evident from the series of oil flow photographs in Fig. 4 and the spanwise pressure distributions shown in Figs. 5 and 6.

Oil Flow

The oil flow patterns of Fig. 4 cover a unit Reynolds number range from 0.86×10^5/in. to 1.2×10^7/in. At the lower Reynolds numbers of Figs. 4a, 4b, and 4c the initial laminar interaction pattern with its widespread separation—oil accumulation at $z/x = 0.87$ or 46° from the axial direction—is clearly visible in the forward corner region and covers the entire wedge surface at the lowest unit Reynolds number. (The curvature of the oil accumulation line in Fig. 4a) is attributed to the effects of the finite span.) The break in the outer oil accumulation line, which occurs at *Re* of approximately $\frac{1}{2} \times 10^6$ (it varied only from 0.47 to 0.55×10^6 over almost two orders of magnitude variation in unit Reynolds number) is attributed to boundary-layer transition triggered by the interaction. Inboard of the oil accumulation line the departure from the purely laminar pattern occurs further upstream due to the earlier perturbation of the boundary layer from interaction with the embedded shock, and therefore, the onset of transition is expected to occur sooner.

The wiggly oil pattern beyond the break, best seen in Fig. 4c), reflects the transition region—*Re* of $\frac{1}{2} \times 10^6$ to approximately $1\frac{1}{2} \times 10^6$. Downstream of this region, the oil pattern shows a typically turbulent interaction which becomes more and more dominant as the unit Reynolds number increases and is considerably narrower than the laminar one—$z/x = 0.45$ or 32° from the axial direction. At the highest unit Reynolds number the laminar and transitional regions are barely visible at the leading edge. Both laminar and turbulent cases, however, reflect an essentially conical flow pattern.

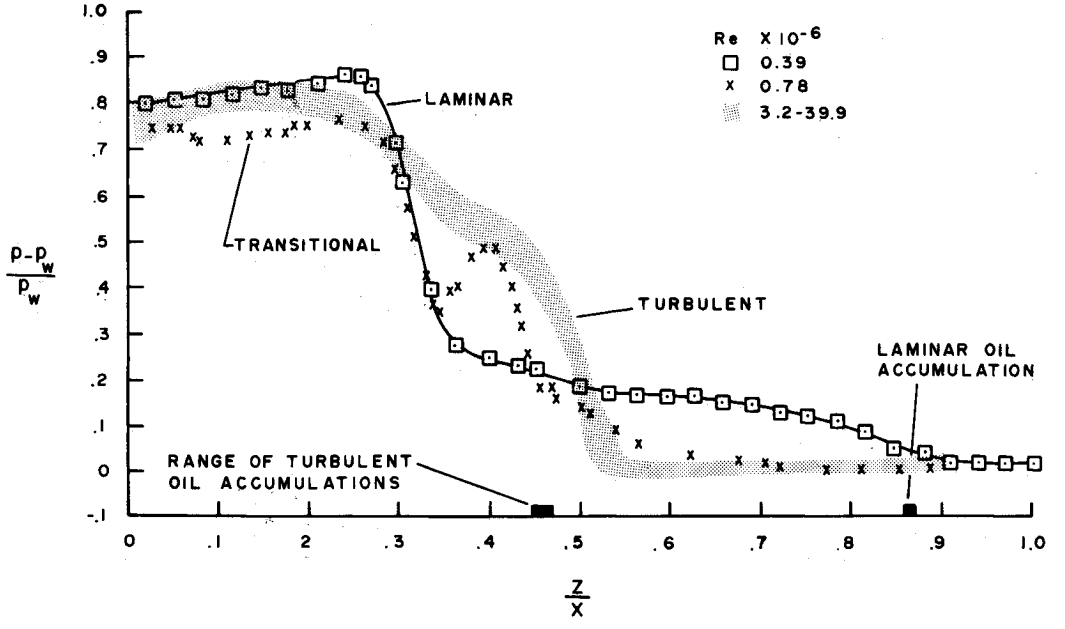

Fig. 6 Surface pressures for a laminar and a transitional case compared with high *Re* data.

In both cases the oncoming streamlines curve into the oil accumulation line—separation. The beginning of curvature reflects the beginning of viscous-inviscid interaction which occurs at $z/x \simeq 0.53$ for the turbulent case and 0.90 for the particular laminar case.

The laminar pattern shows a more pronounced vortical flow than the turbulent case, and strong scavenging action where the oil is virtually wiped clean. This is indicative of high shear and high heat rates as also found in Refs. 1 and 2. The turbulent case shows a weak vortex and a faintly perceptible line of flow divergence—reattachment—separating the almost straight streamlines in the inboard corner region from those directed toward the oil accumulation line.

The considerable difference in the extent of the interaction region between laminar and turbulent flow clearly confirms the viscous nature of the phenomenon. Thus, Region III of Charwat and Redekopp[1] does not occur in the inviscid interaction, but is entirely due to viscous interaction and varies considerably in extent between laminar and turbulent flow. For the latter case, this external region is very small as separation occurs at $z/x = 0.45$ and the position of embedded shock impingement on the wedge is barely smaller (see Fig. 3).

Surface Pressures

Spanwise surface pressure distributions over a range of Re from 3.2 to 39.9 $\times$ 10^6 are remarkably similar and virtually identical within the accuracy of measurement when plotted in nondimensional form as shown in Fig. 5. The laminar interaction near the leading edge appears not to influence the pressure field even at the lowest Re shown. Slight departures in static pressure occur only at the beginning of the sharp pressure rise and reflect a slight spread of the beginning of interaction which grows with decreasing Re, in agreement with the results of the Pitot traverses discussed in the previous section. The positions of oil accumulation which reflect only slight variation with Re, are shown to agree quite well with the first pressure rise with which flow separation is associated. The slight knee in the pressure distribution is followed by a second pressure rise which is associated with flow impingement, or a reattachment line. It agrees well with the position of the faint line of flow divergence noticeable in the oil flow pattern discussed earlier.

A surface pressure distribution obtained at $Re = 0.39 \times 10^6$ and given in Fig. 6 shows a typical laminar configuration similar to those found by previous investigators in supersonic flow[1] and at Mach 20.[2,3] Also shown for comparison is the narrow spread of the sum total of the turbulent data and a pressure distribution obtained in the transition region. The oil accumulation point for the laminar case coincides well with the first pressure rise which begins at $z/x = 0.9$, thus confirming flow lift-off or separation. The second sharp pressure rise at $z/x \simeq 0.3$ coincides with the zone of highly scavenged oil of Fig. 4a, b) and reflects flow impingement, or reattachment.

Similarity with Two-Dimensional Separation

The spanwise surface pressure distributions for laminar and turbulent interaction shown in Fig. 6 have the identical features of those found for two-dimensional separation due to compression ramps or shock wave-boundary layer interactions. For both the axial corner and a two-dimensional configuration, the laminar case is characterized by a large region of separation reflected by the long pressure plateau and followed by a sharp pressure rise at reattachment. The turbulent case is characterized by an initially larger compression following separation, a narrow separated region reflected by the small knee in the pressure distribution, and the reattachment pressure rise. Thus, the viscous-inviscid interaction in supersonic axial corner flow may be viewed as equivalent locally to two-dimensional shock wave boundary-layer interaction with strong cross flow.

Conclusions

The results of an experimental study of flow interaction in a symmetrical axial corner formed by 9.5° intersecting wedges at Mach number 3 and over a range of Re from 0.4 to 60 $\times$ 10^6 show that:

1) Except very near the wedge surfaces, the flow structure is conically invariant for $3 \times 10^6 \leq Re \leq 60 \leq 10^6$ and therefore is considered to represent the inviscid structure.

2) Boundary-layer transition resulted in a considerable decrease in lateral extent of the surface interaction from $z/x = 0.90$ in the laminar region to $z/x = 0.53$ downstream where fully developed turbulent flow existed. The onset of transition in the interaction region occurred at $Re \simeq \frac{1}{2} \times 10^6$ and the extent of the transition region was approximately $\Delta Re \simeq 10^6$.

3) The flow structure and surface pressures varied significantly with Re for values much below 3×10^6; this variation is indicative of the dominant influence of laminar viscous-inviscid interaction and boundary layer displacement effects at relatively low Re, which is also quite evident in the results of Ref. 1.

4) The disturbed region outboard of the embedded shock is entirely due to viscous effects and not of an inviscid nature. Specifically, this region results from flow separation due to the interaction of the embedded shock wave with the boundary layer; the much greater extent of this outer region for laminar than for turbulent flow is typical of the greater spread of separated laminar flow.

5) Spanwise pressure distributions for both the laminar and the turbulent case are virtually identical to those for two-dimensional flow separation so that the former may be viewed locally as two-dimensional shock wave boundary-layer interaction with strong cross-flow.

References

[1] Charwat, A. F. and Redekopp, L. G., "Supersonic Interference Flow along the Corner of Intersecting Wedges," *AIAA Journal*, Vol. 5, No. 3, March 1967, pp. 480–488.

[2] Watson, R. D. and Weinstein, L. M., "A Study of Hypersonic Corner Flow Interactions," *AIAA Journal*, Vol. 9, No. 7, July 1971, pp. 1280–1286.

[3] Bertram, M. H. and Henderson, A. Jr., "Some Recent Research with Viscous Interacting Flow in Hypersonic Streams," *Proceedings of the Symposium on Viscous Interaction Phenomena in Supersonic and Hypersonic Flow*, Hypersonic Research Lab., Aerospace Research Labs., May 1969, pp. 1–30.

[4] Cresci, R. J., Rubin, S. G., Mardo, C. T., and Lin, T. C., "Hypersonic Interaction along a Rectangular Corner," *AIAA Journal*, Vol. 7, No. 12, Dec. 1969, pp. 2241–2246; see also paper Nos. 14 and 18 *AGARD Conference Proceedings No. 30*, May 1968.

[5] Stainback, P. C. and Weinstein, L. M., "Aerodynamic Heating in the Vicinity of Corners at Hypersonic Speeds," TN D-4130, Nov. 1967, NASA.

[6] Korkegi, R. H., "Survey of Viscous Interactions Associated with High Mach Number Flight," *AIAA Journal*, Vol. 9, No. 5, May 1971, pp. 771–784.

[7] Goebel, T. P., "A Theoretical Study of Inviscid Supersonic Flow along a Corner Formed by the Intersection of Two Wedges," Ph.D. thesis, 1969, College of Engineering, Univ. of California, Los Angeles, Calif.

[8] West, J. E. and Korkegi, R. H., "Intersecting Wedges at a Mach number of 3 and High Reynolds Number," ARL 71-0241, Oct. 1971, Aerospace Research Lab., Wright-Patterson Air Force Base, Ohio.